Published in final edited form as:
Mol Cell Neurosci. 2010 January ; 43(1): 81. doi:10.1016/j.mcn.2009.09.006.

KALIRIN LOSS RESULTS IN CORTICAL MORPHOLOGICAL ALTERATIONS

Zhong Xie, **Michael E. Cahill**, and **Peter Penzes***
Department of Physiology, Northwestern University Feinberg School of Medicine, Chicago, IL 60611

Abstract

Morphogenesis of pyramidal neuronal dendrites and spines is crucial for the formation and refinement of forebrain neuronal circuits underlying cognition. Aberrant dendrite and spine morphology is associated with neuropathological disorders. However, the molecular mechanisms controlling pyramidal neuronal dendrite and spine morphogenesis *in vivo* remain largely unknown. Kalirin is a brain-specific guanine-nucleotide exchange factor for Rho-like small GTPases, and an important regulator of spine morphogenesis in cultured neurons. Here we show that RNAi-dependent knockdown of kalirin in cultured neurons affected dendrite morphology. Cortical pyramidal neurons from *KALRN*–null mice showed reduced spine density and impaired activity-dependent spine plasticity; and they exhibited reduced complexity of dendritic trees. *KALRN*–null mice also displayed smaller neuronal cell bodies and reductions in the size of the cortex and cortical layers. These data demonstrate important roles for kalirin in the regulation of cortical structure, ultrastructure, and spine structural plasticity.

Keywords

dendrites; synaptic plasticity; prefrontal cortex; Rac1; knockout; *KALRN*; small GTPase; dendritic spine

INTRODUCTION

On the account that the majority of excitatory synapses on pyramidal neurons in the brain are located on dendrites (Harris, 1999), dendritic spine morphogenesis is cardinal to synaptic development and structural plasticity (Yuste and Bonhoeffer, 2001). Changes in spine structure, number, and shape are important for synapse function during development and plasticity. (Alvarez and Sabatini, 2007; Engert and Bonhoeffer, 1999; Lendvai et al., 2000; Toni et al., 1999). Many cognition-affecting neurodevelopmental, psychiatric, and neurodegenerative disorders are associated with altered dendritic structure and spine morphology. These include schizophrenia (Glantz and Lewis, 2000), Alzheimer's disease (AD) (Falke et al., 2003; Lanz et al., 2003), mental retardation (MR) (Kaufmann and Moser, 2000; Purpura, 1974), and fragile-X syndrome (FraX) (Hinton et al., 1991; Irwin et al., 2000).

Address correspondence to: Peter Penzes, PhD, 303 E Chicago Ave, Ward 7-176, Chicago, IL 60611. Phone: 312-503-5379; Fax: 312-503-5101; p-penzes@northwestern.edu.

The authors declare no conflict of interest.

Pyramidal neurons are the most abundant type of cortical neurons. A feature of these neurons includes a highly branched apical dendrite which receives and integrates signals from superficial cortical layers. The transmission of synaptic signals from dendritic spines to the soma depends on the number of spines, branching pattern and diameter of dendrites, and the distribution of ion channels within the dendritic membrane. Dendrites thus serve as dynamic integrators of synaptic input and greatly affect neuronal information processing (Gulledge et al., 2005; Hausser et al., 2000). Dendritic growth and branching is shaped by neuronal activity through the regulation of the local cytoskeleton via Rho family GTPases, calcium signaling which regulates transcription of genes (Konur and Ghosh, 2005), and membrane trafficking (Ye et al., 2007). Alterations in the morphology of pyramidal neuron dendritic trees have been observed in several neuropsychiatric disorders, including schizophrenia (Black et al., 2004; Broadbelt et al., 2002; Garey et al., 1998; Glantz and Lewis, 2000; Kalus et al., 2000), AD (Falke et al., 2003; Lanz et al., 2003), and MR (Kaufmann and Moser, 2000). These changes, evidenced by a deficiency of neuronal network connectivity, may lead to impaired information processing.

Members of the Rho subfamily of Ras-like small GTPases are central regulators of actin cytoskeletal dynamics in neurons, regulating the development and morphology of dendrites and spines (Nakayama et al., 2000; Tashiro et al., 2000; Threadgill et al., 1997; Wong et al., 2000). Their essential role in regulating spine morphology and human cognition, including learning and memory, is supported by the fact that many types of MR are associated with altered spine morphogenesis. Mutations in genes encoding proteins in the Rho GTPases signaling pathways have also been associated with MR (Dierssen and Ramakers, 2006). Although the role of Rho GTPases in the spine morphogenesis of cultured neurons is relatively well documented, much less is known about their upstream regulators. Guanine-nucleotide exchange factors (GEFs) function as the direct upstream activators of Rho GTPases and are crucial for receptor-mediated regulation of GTPase cascades in cells (Schmidt and Hall, 2002) and neurons (Penzes et al., 2008).

Kalirin is a brain-specific Rho-GEF with several signaling and protein-protein interaction domains (Johnson et al., 2000; Penzes et al., 2000; Penzes and Jones, 2008). Kalirin expression is restricted to specific areas of the brain, (mainly the cerebral cortex and hippocampus) (Ma et al., 2001) and is not detectable outside of the brain. Several alternatively spliced isoforms are generated from the same *KALRN* gene. Kalirin-7 is the most abundant isoform in the adult brain, and is enriched in postsynaptic densities (PSD) of dendritic spines where it controls their morphology (Penzes et al., 2000; Penzes et al., 2001b). The less abundant kalirin isoforms, kalirin-12 and kalirin-9, are localized in the soma, and in the processes and growth cones of young neurons, respectively (Penzes et al., 2001a). The Rac1 activating GEF1 domain of kalirin is present in all isoforms. The GEF2 domain, present only in kalirin-9 and kalirin-12, activates RhoA (Penzes et al., 2001a). While kalirin-9 and -12 are expressed early-on during postnatal development, kalirin-7 expression finally surpasses the detection threshold as Kalirin-9 and -12 expression become reduced, after P7-10 (Ma et al., 2003; Xie et al., 2007). We have recently shown that kalirin plays an important role in activity-dependent spine enlargement, synaptic expression and maintenance of AMPA receptors (AMPAR), and AMPAR-mediated synaptic transmission (Xie et al., 2007). In addition, we have demonstrated a role for kalirin-7 in the modulation of spine morphology by the trans-synaptic adhesion molecule N-cadherin in cortical pyramidal neurons (Xie et al., 2008).

While the phenotypic effects of removing the exon specific for the kalirin-5 and -7 isoforms have recently been investigated (Ma et al., 2008), the effects of removing the entire kalirin gene on cortical morphology is not known. We have recently reported the generation of a *KALRN*-null (KO) mouse, which exhibited a working memory deficit (Cahill et al., 2009). We hypothesized that kalirin ablation may lead to impairment in both spine and dendrite

morphogenesis *in vivo* and that this aberrant cortical spine and dendrite morphology may be associated with cognitive behavior dysfunction. To test this, we analyzed cortical structure and ultrastructure in *KALRN*-KO mice. We found that cortical pyramidal neurons from KO mice had reduced spine density, altered dendrite morphology, and impaired spine structural plasticity. KO mice showed reduced dendritic branching and complexity in native tissue. These effects were similar to those caused by RNAi-mediated knockdown of kalirin. In addition, KO mice exhibited cortical layer-specific alterations in the size of neuronal cell bodies and layer thickness. This data demonstrates that kalirin is important in regulating cortical morphology.

RESULTS

Knockdown of kalirin resulted in altered dendritic morphology in cultured pyramidal neurons

While kalirin has been shown to regulate dendritic spine morphology, its role in regulating dendrite maintenance in mature neurons has not been studied. To determine whether loss of kalirin in neurons with mature morphologies affected dendrite morphology at the level of individual neurons, we knocked down kalirin expression in cultured neurons with RNA interference (RNAi) treatment. This approach efficiently and specifically knocked down kalirin expression in cultured neurons, and kalirin loss led to spine loss (Xie et al., 2007). We found that kalirin knock-down in mature cortical pyramidal neurons (DIV 28) resulted in a reduction of dendritic branching, determined by the number of dendritic terminal points; this effect was time-dependent and progressive, as shorter knockdown period resulted in a partial reduction in dendritic terminal points (Fig. 1A–B; control 51.2±6.1, 3-day RNAi 26.4±4.5, 5-day RNAi 14.3±2.9). The primary, secondary, and tertiary dendrites were traced and analysis demonstrated that the reductions of dendrite branching and total dendritic length were primarily due to reduced tertiary dendrite branches and length (Fig. 1C, 1D; Fig. S1).

Spine loss, impaired activity-dependent spine plasticity in pyramidal neurons of KALRN KO mice

Kalirin has been shown to regulate spine numbers and spine morphology cultured pyramidal neurons (Penzes et al., 2003; Penzes et al., 2001b; Penzes and Jones, 2008; Xie et al., 2007); however, the effects of complete *KALRN* gene ablation on spine morphology and structural plasticity have not been accessed. To this end, we generated *KALRN* KO mice (Fig. S2A). These mice lack the expression of all kalirin isoforms. Detailed description of the *KALRN* KO mice was reported recently (Cahill et al., 2009). At 4 weeks of age, KO mice weighed significantly less than wild type littermates (WT) (WT 12.0±0.3g, KO 10.5±0.3g, $p<0.05$). However, this difference decreased as they grew (Fig. S2B); and by 12~16 weeks of age there was no significant difference in body weight (WT 22.5±1.9g, KO 20.5±1.6g, $p=0.06$). Analysis of Golgi staining and two-photon laser scanning microscopy revealed significant spine loss in the cortex of KO animals compared to WT controls (Cahill et al., 2009). Consistent with the *in vivo* findings, similar reduction in spine density was observed in cultured cortical pyramidal neurons originated from KO mice (WT 9.92±0.75, KO 6.55±0.50 spines/10 μm, $p<0.05$); no significant changes were found in spine area, breadth and length (Fig. 2A, 2B).

Our previous studies demonstrated that kalirin regulates activity-dependent structural and functional plasticity in cultured cortical pyramidal neurons; we found that kalirin-7 controls synaptic expression and maintenance of AMPAR, and AMPAR-mediated synaptic transmission (Xie et al., 2007). Activity-dependent modifications of central excitatory synapses are crucial for synapse maturation, synaptic plasticity, and information processing and storage (Malinow, 2003; Yuste and Bonhoeffer, 2001). Activation of NMDA receptor results in the ion channel opening of this ionotropic glutamate receptor. To examine whether NMDA receptor (NMDAR) activation-dependent spine plasticity and AMPAR delivery to spines was affected by the absence of kalirin, we compared cultured cortical neurons from KO and WT

mice. The cultures were maintained in media containing 200 μM competitive NMDAR antagonist APV (amino-phosphonovalerate) starting from DIV 4 and were used at DIV 28. Thirty minutes after NMDAR activation by APV withdrawal, WT neurons showed marked increase in spine size and spine content of the AMPAR GluR1 subunit, while no significant changes were found in these measurements in KO neurons subjected to NMDAR activation (Fig. 2A~C). These findings suggest impairment of activity-dependent spine plasticity in *KALRN* KO neurons.

Dendritic structure alterations in cortical pyramidal neurons of KALRN KO mice

Dendritic growth and branching is shaped by Rho family GTPases (Konur and Ghosh, 2005); and kalirin is a GEF for these proteins (Penzes et al., 2001b). In mature cultured cortical neurons, kalirin knock down resulted in impaired dendritic morphology (Fig. 1). We next examined dendrite morphology in the cortex of *KALRN* KO mice. The fine morphology of dendritic structures on pyramidal neurons in the neocortex was revealed by Golgi staining (Fig. S3) (Elia et al., 2006). Brains of 3-month-old male KO and WT littermate pairs were processed in parallel. High magnification images showed markedly reduced dendritic complexity in KO mice (Fig. 3A). To quantitatively analyze changes in dendritic structures, layer 5 pyramidal neurons were traced with Neurolucida and analyzed using Neurolucida Explorer. Representative 2D projections of the tracings were shown in Fig. 3B. Dendritic branching, reflected by total number of terminal branching points (Fig. 3C; WT 36.2±2.3, KO 19.0±0.6; $p<0.01$), as well as total apical dendritic length (Fig. 3D; WT 2082±316 μm, KO 978±97 μm; $p<0.05$), were greatly reduced in layer 5 pyramidal neurons of KO mice. Sholl analysis on these neurons also revealed reduced dendrite complexity in both the apical dendritic tree (Fig. 3E) and the basal dendritic trees (Fig. 3F) in the *KALRN* KO mice compared with their WT littermates.

Dendritic structure alterations in cultured KALRN KO pyramidal neurons

To determine whether any difference in dendritic morphology existed between neurons in native tissue and in culture, dendritic morphology was evaluated in cortical neuron cultures originated from neonatal KO and WT mice and grown for 4 weeks (Penzes et al., 2003). Neurons were transfected with GFP to allow high-resolution imaging of dendritic and spine structures with confocal microscopy. Pyramidal neurons from KO mice had fewer dendritic branches (Fig. 4A, 4B; WT 52.2±3.1, KO 37.7±1.6; $p<0.001$). These results, combined with similar effects of kalirin RNAi treatment on mature neurons, demonstrated that the effects of kalirin loss occur directly at the level of individual neurons, not a secondary effect from some unknown systemic changes.

Cytoarchitectural alterations in the frontal cortex of KALRN KO mice

To determine whether knocking out kalirin affected frontal cortical cytoarchitecture, we performed histochemical staining with Nissl or eosin/hematoxylin reagents on sagittal brain sections of 3-month-old *KALRN* KO mice and WT littermates. We found in the KO mice a significant decrease in neuron soma size (Fig. 5A–B; WT 207.2±14.5, KO 149.8±6.4 μm^2; $p<0.05$) and an increase in neuron density (Fig. 5A, 5C; WT 8.8±1.2, KO 10.8±1.0 cells/10000 μm^2; $p<0.05$) in layer 5, whereas no changes were found in other frontal cortical layers. The decrease in soma size in KO layer 5 was a result of a distribution shift of larger soma (most likely pyramidal neurons) toward smaller sizes (Fig. S4A). In comparison, in layer 2/3, the distribution of soma sizes of KO mice was not changed from that of the WT littermates (Fig. S4B).

Cortical macroanatomical changes in KALRN KO mice

We then compared the gross morphology of the brains WT and KO mice to determine whether knocking out kalirin resulted in major anatomical modifications in the brain. For detailed analysis, we examined sagittal brain sections of 3-month-old WT and KO littermate mice by wide-field microscopy. The cerebral cortex of KO mice was slightly smaller than that of the WT littermates (Fig. 6A, 6B; KO was 90.3±0.6% of WT littermates, $p<0.01$). In contrast, the size of the cerebellum was not altered (KO was 99.8±0.3% of WT littermates, $p=0.87$). We next analyzed the laminar structures in the cortex of *KALRN* KO mice, specifically in the frontal cortex. The black rectangular boxes in Fig. 6A indicate the cortex areas analyzed. The overall cortical thickness, measured at the level of frontal cortex, was reduced in KO mice (Fig. 6C, 6D; WT 1688±81 μm, KO 1574±68 μm; $p<0.05$). Among the cortical layers, layer 5 showed significant reduction in thickness compared to WT littermates (Fig. 6C, 6D; WT 616±30 μm, KO 543±21 μm; $p<0.01$).

DISCUSSION

In this study we report that loss of kalirin resulted in cortical pyramidal neurons having reduced spine density and spine plasticity, as well as reduced dendritic branching and dendritic length, both *in vitro* and *in vivo*. These changes occurred at the individual neuronal level. Mice with a full KO of the *KALRN* gene showed reduced cerebral cortex size but otherwise normal brain macroanatomy. The overall thickness of the frontal cortex was reduced, in large part due to a thinner layer 5. Among the laminar layers in the frontal cortex, layer 5 pyramidal neurons exhibited a decrease in soma size and an increase in neuron density, presumably reflecting increased cell packing due to reductions in both cell body size and dendrite branching. Taken together, these data support a role for kalirin in regulating the morphology of cortical pyramidal neurons and the frontal cortex.

The *KALRN* gene produces several kalirin isoforms generated by alternative splicing. It has been shown previously that kalirin-7, highly enriched in dendritic spines, is important in dendritic spine maintenance and plasticity in mature neurons (Penzes et al., 2001b; Xie et al., 2007), and kalirin-9 is important in neurite growth and neuronal morphology in young neurons (Penzes et al., 2001a). A recent study examined mice with a deletion of the exon encoding a short peptide targeting kalirin-7 to spines (Ma et al., 2008). The removal of the exon encoding the C-terminus of kalirin-7 resulted in compensatory upregulation of the non-synaptic kalirin-8, -9 and -12 isoforms, and an approximate 25% reduction in total forebrain kalirin protein in the Δkalirin-7 mice. Interestingly, *KALRN* KO mice exhibit some features similar to the Δkalirin-7 mice, in that they are viable, fertile, have no obvious defects in gross anatomy, and show normal mobility and sensory perception (Cahill et al., 2009). Cortical cultures from both Δkalirin-7 and *KALRN* KO mice showed reduced spine density. However, while cortical spine density was reduced *in vivo* in *KALRN* KO mice (Cahill et al., 2009), spine density in cortical tissue from Δkalirin-7 mice has not been reported.

Kalirin isoforms exhibit distinct and overlapping localization patterns, expression timelines, and regulatory effects on spine morphology and neurite development. Expression of kalirin-9 and kalirin-12 predominates in the neonatal cortex, while Kalirin-7 expression only emerges around P7-10. Kalirin-9 is enriched in processes and growth cones of cortical neurons. Kalirin-9 exerts a dramatic effect on neurite length and neuronal morphology, implicating its importance in neuritogenesis. On the other hand, the late expression onset of kalirin-7 implies a role in dendrite and spine maintenance. *KALRN* KO mice were designed to be deficient in all kalirin forms, preventing possible compensatory effects (Cahill et al., 2009). Consequently, *KALRN* KO mice demonstrated deficits in both spine density and dendritic growth, mimicking the aberrant neuronal morphology in both dendritic arbor and dendritic spines prominent in many neuropsychiatric disorders.

Kalirin is a GEF for small GTPases Rac1 and RhoA (Penzes et al., 2001b; Penzes and Jones, 2008). Rho family GTPases play important roles in the regulation of neuronal network formation, including neurite outgrowth, polarity, axon guidance, dendritic development and synapse formation. Among Rho family GTPases, Rac and Cdc42 promote dendrite growth and branching and axon elongation, Rho acts as a negative regulator for dendrite and axon growth (Penzes et al., 2008). A few other Rho/Rac GEFs have been shown to affect dendrite morphology: Tiam1 (a Rac1 GEF) promotes dendritic arbor growth in cultured neurons (Tolias et al., 2007); and Lfc (a Rho GEF) expression results in reduction in spine length and size (Ryan et al., 2005). In addition, various forms of MR have been linked to genes encoding components directly involved in Rho GTPases signaling pathways. These genes include *OPHN1*, *PAK-3* and *ARHGEF6* in nonsyndromic X-linked MR; *OCRL1* and *FMR1* in syndromic X-linked MR; *LIMK1* and *MEGAP* in autosomal syndromic MR (Benarroch, 2007; Negishi and Katoh, 2002).

Kalirin has been previously investigated as a regulator of spine morphogenesis. We found in the present study that it also regulates the morphogenesis and maintenance of the dendritic trees. In addition to reduced dendritic branching and complexity, cortical pyramidal neurons in *KALRN* KO mice showed substantial spine loss (Fig. 2~4). Blocking kalirin expression through RNA interference blocked activity-dependent plasticity in cultured cortical pyramidal neurons (Xie et al., 2007). Consistent with that finding, we show here that ablation of kalirin resulted in deficit in activity-dependent spine plasticity: compared with pyramidal neurons from WT mice, *KALRN* KO neurons exhibited no NMDAR activation-induced spine enlargement or AMPAR clustering in spines (Fig. 2).

Dendritic spine loss, aberrant spine/dendrite morphology are prominent features of some neurodevelopmental and neuropsychiatric disorders, such as MR, AD, DS, and schizophrenia, where cognitive functions are affected (Sweet et al., 2009). It is thus of great interest to learn whether loss of an important regulator of spine and dendrite morphogenesis, kalirin, resulted in any deficit in learning and memory behavior. Indeed, in a recent study, we found *KALRN* KO mice exhibited marked impairment in spatial working memory in Morris water maze and Y-maze tasks, while spatial reference memory was intact (Cahill et al., 2009). Since reference memory is more hippocampal-dependent and working memory requires the integrity of network connections within the prefrontal cortex and between prefrontal cortex and hippocampus (Goldman-Rakic, 1995; Yoon et al., 2008), we focused this study on the structure and ultrastructure of the frontal cortex. Our findings support the notion that kalirin is an important regulator of spine and dendrite morphology in the cerebral cortex; and cognitive dysfunction may result from aberrant dendrite and spine morphology.

We also detected unexpected and specific cytoarchitectural and brain macroanatomical alterations in *KALRN* KO mice. The role of Rho GTPase signaling in the regulation of cortical pyramidal neuronal soma size and cortical layer thickness has not yet been extensively explored. *KALRN* KO mice showed cortical layer-specific reduction in neuronal size, increase in cell density, and reduction in layer thickness. Interestingly, reduced pyramidal cell body size, increased cell density, and reduced cortical thickness have all been reported in schizophrenia (Sweet et al., 2004).

Recent studies on human subjects suggest potential roles for kalirin signaling in several neuropsychiatric disorders. Reduced expression of kalirin mRNA has been detected in the prefrontal cortex of subjects with schizophrenia (Hill et al., 2006; Narayan et al., 2008), and these reduced kalirin transcript levels correlated strongly with spine loss in the schizophrenia frontal cortex irrespective of antipsychotic treatment (Hill et al., 2006). Kalirin directly interacts with schizophrenia susceptibility gene DISC1 (Disrupted-in-Schizophrenia-1) (Millar et al., 2003). Analysis of postmortem brain tissue found that in human subjects with

AD, kalirin mRNA and protein were consistently underexpressed (Youn et al., 2007a). In addition, kalirin also interacts with Huntingtin-associated protein 1, which is potentially interesting as morphological alterations of dendrites and spines occur in HD and in animal models of HD (Yasuda et al., 1995; Youn et al., 2007b).

EXPERIMENTAL METHODS

Reagents

GluR1 polyclonal antibody was a gift from the Huganir laboratory (John's Hopkins University) and was used at 1:400 dilution for immunofluorescence. This antibody was raised against the carboxy terminus peptide of rat GluR1 and showed no cross-reaction with GluR2–4. It also recognizes GluR1 in several other species (e.g., mouse, human). GFP monoclonal antibody was purchased from Chemicon and used at 1:1000 dilution for immunofluorescence. Constructs for GFP expression and kalirin knockdown were described in detail previously (Xie et al., 2008; Xie et al., 2007). The kalirin knockdown construct was derived from a pGsuper plasmid which simultaneously expresses EGFP and small hairpin RNA (shRNA) for RNA interference. The target for RNA interference is nucleotides 1229–1250 (sequence: GCAGTACAATCCTGGCCATGT) on the KALRN gene, which is common to kalirin7, kalirin9 and kalirin12. D,L-amino-phosphonovalerate (APV) was purchased from Ascent Scientific.

Generation of the *KALRN*-null mice

Design and generation of the *KALRN* null mice has been described in detail previously (Cahill et al., 2009). Briefly, a targeting construct was designed in which exons 27–28 was replaced by the neo cassette under an independent PGK promoter. The PGK-neo cassette was inserted in reverse orientation and contained a loxP sites at each end to allow for excision. *KALRN* null mice were generated from ES cells by inGenious Targeting Laboratory (Stony Brook, NY) using standard methods. PCR analysis using WT and KO-specific primers indicated that the *KALRN* gene was disrupted. No kalirin proteins were detected by Western blotting of brain homogenates.

Dissociated cultures of primary neurons

Primary neuronal cultures were generated from cerebral cortices of either E18 embryos (for RNA interference experiments) or P1 pups (for KO and WT comparison experiments) of C57BL/6 mice, and cultured *in vitro* in Neurobasal media supplemented with B27 (Invitrogen), as described previously (Xie et al., 2007). P1 pups were used for KO and WT comparison experiments so the mothers can be saved for breeding purpose. To examine dendrite and spine morphologies, neurons were transfected with GFP expressing construct, fixed with 3.7% formaldehyde in PBS containing 10% sucrose for 20 min at room temperature, and immunostained with a GFP monoclonal antibody (Chemicon; 1:1000 dilution). Neuron transfections were performed with the specified DNA constructs and Lipofectamine 2000 (Invitrogen) according to manufacturer's instruction (Penzes et al., 2003). APV withdrawal treatment was carried out as detailed previously (Xie et al., 2007).

Image acquisition and immunofluorescence analysis

Visualization and quantification of dendrite and spine morphologies were performed as described in (Xie et al., 2007). Briefly, neurons with healthy, typical pyramidal morphologies were imaged with a Zeiss LSM5 Pascal confocal microscope. Detector gain and offset were adjusted to include all spines, and Z-stacks of images were taken with a 63x objective. Experiments were done blind to conditions and on sister cultures. Cultures that were directly compared were imaged with the same acquisition parameters. An anti-GFP antibody was used

to circumvent potential unevenness of GFP diffusion in spines. Neurons with comparable, medium GFP fluorescence intensity were imaged. Individual spines were outlined on reconstructed 2D images and morphological parameters (linear density: number of spines per 10 μm of dendrite; area: area of the perimeter enclosed by the outline of the spine; length: the distance from the base to the tip of the spine; breadth: the maximum width of the spine) were measured using Metamorph software (Molecular Devices, Downingtown, PA). Neuronal expression and localization of GluR1 were visualized with immunofluorescence and quantified using MetaMorph. Images were acquired as described above. The background corresponding to areas without cells were subtracted to generate a "background-subtracted" image. To measure the intensity of GluR1 clusters localized within spines, regions defining spines were generated based on GFP fluorescence in one channel. These regions were then transferred to the GluR1 fluorescence channel, and only the GluR1 fluorescence integrated intensities within the corresponding spine regions were measured. Dendritic morphological parameters (dendritic lengths, number of dendritic tips) were quantified with NIH imageJ. Nine to twelve cells each group from at least two separate experiments were analyzed.

Histology

Brains of 3-month-old male littermate KO and WT mice were fixed in 4% paraformaldehyde, embedded in paraffin, and sagittally sectioned into 4 μm sections. Each littermate pair of KO and WT mice brains was embedded in the same paraffin block, sectioned and processed in parallel. Three pairs of male littermate KO and WT mice brains were analyzed. Staining procedures were carried out according to standard protocols. Nissl staining: sections were deparaffinized in xylene and rehydrated, stained in 0.1% cresyl violet for 5 min, quickly rinsed in distilled water and differentiated in ethanol, dehydrated, cleared in xylene, and mounted with Permount. Hematoxylin & Eosin (H&E) Staining: sections were deparaffinized in xylene and rehydrated, stained in Mayer hematoxylin solution (0.1%) for 8 min, washed and counterstained in eosin Y solution (0.25%) for 1 min; sections were then dehydrated, cleared in xylene, and mounted with Permount.

Size measurements and neuron counting

Images of stained brain sagittal sections were acquired by a Zeiss Axioplan 2 microscope, processed and quantified with the Metamorph software. The borders of the cerebral cortex and cerebellum, and the borders of the frontal cortical layers were identified by comparing acquired images with the Allen Mouse Brain Reference Atlas (http://mouse.brain-map.org/atlas/index.html). For cerebral cortex and cerebellar measurements, the target brain areas were outlined, highlighted, and measured. The thicknesses of frontal cortical layers were measured perpendicular to the cortex surface. Cell number and soma size quantification was done on Nissl stained images as follow: a vertical rectangular region as shown in Fig 6A was chosen; the previously identified cortical layer borders were drawn to separate the whole cortical region into four sub-regions, i.e., layer 1, 2/3, 5, and 6; for each layer region, the image was threshold to just highlight the dark soma in that layer (soma were mostly separate, in some case when neighboring soma were in contact they were manually divided). Areas above threshold but smaller than 50 μm^2 were not counted as soma. The area of the layer region, number of cells within the region, and the areas of every cell body were quantified automatically in Metamorph; for those cells on the borders, only cells touching the top and left borders were counted. Three pairs of WT and KO littermate brains were analyzed. For each brain, four laterally equal-spaced sections 0.6mm apart were analyzed. All measurements and comparisons were made on brain sections of the same sagittal coordination based on the Allen Mouse Brain Reference Atlas.

Golgi staining

Golgi taining was performed using modified Golgi-Cox impregnation method. Brains of 3-month-old male littermate KO and WT mice were processed in parallel and stained with a FD Rapid GolgiStain kit (FD NeuroTechnologies, Ellicott City, MD) following the manufacturer's protocol. High and low magnification images were taken by a Zeiss Axioplan 2 microscope. To analyze dendritic morphology, Golgi-stained pyramidal neurons were manually traced with Neurolucida (MicroBrightField, Williston, VT); total dendritic length and number of dendritic tips (a measure of branching) were measured and quantified using Neurolucida Explorer. Sholl analysis was also performed with Neurolucida Explorer to demonstrate the branching patterns of the neuronal dendritic trees. Briefly, concentric circles with gradually increasing radius centered at the centroid of the cell body were drawn, and the numbers the neuron intersects with the circumferences of these circles were counted and plotted. Three pairs of male WT and KO littermate brains were analyzed. For each brain, Two to three layer 5 pyramidal neurons from the frontal cortex were traced.

Statistics

All data represent means ± SEM. Statistical analyses for two group comparison were done with Student's *t* test; paired samples *t* test was used when results from matched WT and KO littermates were compared. One-way ANOVA followed by *post hoc* Tukey's multiple-comparison test was used to determine the statistical significance of the differences among multiple groups (GraphPad Prism). Differences were deemed statistically significant when $p < 0.05$.

Supplementary Material

Refer to Web version on PubMed Central for supplementary material.

Acknowledgments

We thank Dr. Richard L. Huganir (Johns Hopkins University) for the GluR1 polyclonal antibody; Dr. Gary G. Borisy and Dr. Shin-ichiro Kojima (Northwestern University) for the pGsuper plasmid and assistance with RNAi; and Kelly Jones and Igor Rafalovich for editing. This work was supported by grants from NIH-NIMH (R01MH071316), National Alliance for Autism Research (NAAR), National Alliance for Research on Schizophrenia and Depression (NARSAD), and Alzheimer's Association (to P.P.), and training grants (NINDS 5T32NS041234-08) to Z.X. and (NIH 1F31AG031621-01A2) to M.E.C.

REFERENCES

Alvarez VA, Sabatini BL. Anatomical and physiological plasticity of dendritic spines. Annual review of neuroscience 2007;30:79–97.

Benarroch EE. Rho GTPases: role in dendrite and axonal growth, mental retardation, and axonal regeneration. Neurology 2007;68:1315–1318. [PubMed: 17438224]

Black JE, Kodish IM, Grossman AW, Klintsova AY, Orlovskaya D, Vostrikov V, Uranova N, Greenough WT. Pathology of layer V pyramidal neurons in the prefrontal cortex of patients with schizophrenia. The American journal of psychiatry 2004;161:742–744. [PubMed: 15056523]

Broadbelt K, Byne W, Jones LB. Evidence for a decrease in basilar dendrites of pyramidal cells in schizophrenic medial prefrontal cortex. Schizophrenia research 2002;58:75–81. [PubMed: 12363393]

Cahill M, Xie Z, Day M, Barbolina M, Miller C, Weiss C, Radulovic J, Sweatt D, Disterhoft J, Surmeier D, Penzes P. Kalirin regulates cortical spine morphogenesis and disease-related behavioral phenotypes. PNAS. 2009 in press.

Dierssen M, Ramakers GJ. Dendritic pathology in mental retardation: from molecular genetics to neurobiology. Genes, brain, and behavior 2006;5:48–60.

Elia LP, Yamamoto M, Zang K, Reichardt LF. p120 catenin regulates dendritic spine and synapse development through Rho-family GTPases and cadherins. Neuron 2006;51:43–56. [PubMed: 16815331]

Engert F, Bonhoeffer T. Dendritic spine changes associated with hippocampal long-term synaptic plasticity. Nature 1999;399:66–70. [PubMed: 10331391]

Falke E, Nissanov J, Mitchell TW, Bennett DA, Trojanowski JQ, Arnold SE. Subicular dendritic arborization in Alzheimer's disease correlates with neurofibrillary tangle density. The American journal of pathology 2003;163:1615–1621. [PubMed: 14507668]

Garey LJ, Ong WY, Patel TS, Kanani M, Davis A, Mortimer AM, Barnes TR, Hirsch SR. Reduced dendritic spine density on cerebral cortical pyramidal neurons in schizophrenia. Journal of neurology, neurosurgery, and psychiatry 1998;65:446–453.

Glantz LA, Lewis DA. Decreased dendritic spine density on prefrontal cortical pyramidal neurons in schizophrenia. Archives of general psychiatry 2000;57:65–73. [PubMed: 10632234]

Goldman-Rakic PS. Cellular basis of working memory. Neuron 1995;14:477–485. [PubMed: 7695894]

Gulledge AT, Kampa BM, Stuart GJ. Synaptic integration in dendritic trees. Journal of neurobiology 2005;64:75–90. [PubMed: 15884003]

Harris KM. Structure, development, and plasticity of dendritic spines. Current opinion in neurobiology 1999;9:343–348. [PubMed: 10395574]

Hausser, M.; Spruston, N.; Stuart, GJ. Science. Vol. 290. New York, N.Y: 2000. Diversity and dynamics of dendritic signaling; p. 739-744.

Hill JJ, Hashimoto T, Lewis DA. Molecular mechanisms contributing to dendritic spine alterations in the prefrontal cortex of subjects with schizophrenia. Molecular psychiatry 2006;11:557–566. [PubMed: 16402129]

Hinton VJ, Brown WT, Wisniewski K, Rudelli RD. Analysis of neocortex in three males with the fragile X syndrome. American journal of medical genetics 1991;41:289–294. [PubMed: 1724112]

Irwin SA, Galvez R, Greenough WT. Dendritic spine structural anomalies in fragile-X mental retardation syndrome. Cereb Cortex 2000;10:1038–1044. [PubMed: 11007554]

Johnson RC, Penzes P, Eipper BA, Mains RE. Isoforms of kalirin, a neuronal Dbl family member, generated through use of different 5'- and 3'-ends along with an internal translational initiation site. The Journal of biological chemistry 2000;275:19324–19333. [PubMed: 10777487]

Kalus P, Muller TJ, Zuschratter W, Senitz D. The dendritic architecture of prefrontal pyramidal neurons in schizophrenic patients. Neuroreport 2000;11:3621–3625. [PubMed: 11095531]

Kaufmann WE, Moser HW. Dendritic anomalies in disorders associated with mental retardation. Cereb Cortex 2000;10:981–991. [PubMed: 11007549]

Konur S, Ghosh A. Calcium signaling and the control of dendritic development. Neuron 2005;46:401–405. [PubMed: 15882639]

Lanz TA, Carter DB, Merchant KM. Dendritic spine loss in the hippocampus of young PDAPP and Tg2576 mice and its prevention by the ApoE2 genotype. Neurobiology of disease 2003;13:246–253. [PubMed: 12901839]

Lendvai B, Stern EA, Chen B, Svoboda K. Experience-dependent plasticity of dendritic spines in the developing rat barrel cortex in vivo. Nature 2000;404:876–881. [PubMed: 10786794]

Ma XM, Huang J, Wang Y, Eipper BA, Mains RE. Kalirin, a multifunctional Rho guanine nucleotide exchange factor, is necessary for maintenance of hippocampal pyramidal neuron dendrites and dendritic spines. J Neurosci 2003;23:10593–10603. [PubMed: 14627644]

Ma XM, Johnson RC, Mains RE, Eipper BA. Expression of kalirin, a neuronal GDP/GTP exchange factor of the trio family, in the central nervous system of the adult rat. The Journal of comparative neurology 2001;429:388–402. [PubMed: 11116227]

Ma XM, Kiraly DD, Gaier ED, Wang Y, Kim EJ, Levine ES, Eipper BA, Mains RE. Kalirin-7 is required for synaptic structure and function. J Neurosci 2008;28:12368–12382. [PubMed: 19020030]

Malinow R. AMPA receptor trafficking and long-term potentiation. Philosophical transactions of the Royal Society of London 2003;358:707–714. [PubMed: 12740116]

Millar JK, Christie S, Porteous DJ. Yeast two-hybrid screens implicate DISC1 in brain development and function. Biochemical and biophysical research communications 2003;311:1019–1025. [PubMed: 14623284]

Nakayama AY, Harms MB, Luo L. Small GTPases Rac and Rho in the maintenance of dendritic spines and branches in hippocampal pyramidal neurons. J Neurosci 2000;20:5329–5338. [PubMed: 10884317]

Narayan S, Tang B, Head SR, Gilmartin TJ, Sutcliffe JG, Dean B, Thomas EA. Molecular profiles of schizophrenia in the CNS at different stages of illness. Brain research. 2008

Negishi M, Katoh H. Rho family GTPases as key regulators for neuronal network formation. Journal of biochemistry 2002;132:157–166. [PubMed: 12153710]

Penzes P, Beeser A, Chernoff J, Schiller MR, Eipper BA, Mains RE, Huganir RL. Rapid induction of dendritic spine morphogenesis by trans-synaptic ephrinB-EphB receptor activation of the Rho-GEF kalirin. Neuron 2003;37:263–274. [PubMed: 12546821]

Penzes P, Cahill ME, Jones KA, Srivastava DP. Convergent CaMK and RacGEF signals control dendritic structure and function. Trends in cell biology 2008;18:405–413. [PubMed: 18701290]

Penzes P, Johnson RC, Alam MR, Kambampati V, Mains RE, Eipper BA. An isoform of kalirin, a brain-specific GDP/GTP exchange factor, is enriched in the postsynaptic density fraction. The Journal of biological chemistry 2000;275:6395–6403. [PubMed: 10692441]

Penzes P, Johnson RC, Kambampati V, Mains RE, Eipper BA. Distinct roles for the two Rho GDP/GTP exchange factor domains of kalirin in regulation of neurite growth and neuronal morphology. J Neurosci 2001a;21:8426–8434. [PubMed: 11606631]

Penzes P, Johnson RC, Sattler R, Zhang X, Huganir RL, Kambampati V, Mains RE, Eipper BA. The neuronal Rho-GEF Kalirin-7 interacts with PDZ domain-containing proteins and regulates dendritic morphogenesis. Neuron 2001b;29:229–242. [PubMed: 11182094]

Penzes P, Jones KA. Dendritic spine dynamics--a key role for kalirin-7. Trends in neurosciences 2008;31:419–427. [PubMed: 18597863]

Purpura DP. Dendritic spine "dysgenesis" and mental retardation. Science (New York, N. Y 1974;186:1126–1128.

Ryan XP, Alldritt J, Svenningsson P, Allen PB, Wu GY, Nairn AC, Greengard P. The Rho-specific GEF Lfc interacts with neurabin and spinophilin to regulate dendritic spine morphology. Neuron 2005;47:85–100. [PubMed: 15996550]

Schmidt A, Hall A. Guanine nucleotide exchange factors for Rho GTPases: turning on the switch. Genes & development 2002;16:1587–1609. [PubMed: 12101119]

Sweet RA, Bergen SE, Sun Z, Sampson AR, Pierri JN, Lewis DA. Pyramidal cell size reduction in schizophrenia: evidence for involvement of auditory feedforward circuits. Biological psychiatry 2004;55:1128–1137. [PubMed: 15184031]

Sweet RA, Henteleff RA, Zhang W, Sampson AR, Lewis DA. Reduced dendritic spine density in auditory cortex of subjects with schizophrenia. Neuropsychopharmacology 2009;34:374–389. [PubMed: 18463626]

Tashiro A, Minden A, Yuste R. Regulation of dendritic spine morphology by the rho family of small GTPases: antagonistic roles of Rac and Rho. Cereb Cortex 2000;10:927–938. [PubMed: 11007543]

Threadgill R, Bobb K, Ghosh A. Regulation of dendritic growth and remodeling by Rho, Rac, and Cdc42. Neuron 1997;19:625–634. [PubMed: 9331353]

Tolias KF, Bikoff JB, Kane CG, Tolias CS, Hu L, Greenberg ME. The Rac1 guanine nucleotide exchange factor Tiam1 mediates EphB receptor-dependent dendritic spine development. Proceedings of the National Academy of Sciences of the United States of America 2007;104:7265–7270. [PubMed: 17440041]

Toni N, Buchs PA, Nikonenko I, Bron CR, Muller D. LTP promotes formation of multiple spine synapses between a single axon terminal and a dendrite. Nature 1999;402:421–425. [PubMed: 10586883]

Wong WT, Faulkner-Jones BE, Sanes JR, Wong RO. Rapid dendritic remodeling in the developing retina: dependence on neurotransmission and reciprocal regulation by Rac and Rho. J Neurosci 2000;20:5024–5036. [PubMed: 10864960]

Xie Z, Photowala H, Cahill ME, Srivastava DP, Woolfrey KM, Shum CY, Huganir RL, Penzes P. Coordination of synaptic adhesion with dendritic spine remodeling by AF-6 and kalirin-7. J Neurosci 2008;28:6079–6091. [PubMed: 18550750]

Xie Z, Srivastava DP, Photowala H, Kai L, Cahill ME, Woolfrey KM, Shum CY, Surmeier DJ, Penzes P. Kalirin-7 controls activity-dependent structural and functional plasticity of dendritic spines. Neuron 2007;56:640–656. [PubMed: 18031682]

Yasuda RP, Ikonomovic MD, Sheffield R, Rubin RT, Wolfe BB, Armstrong DM. Reduction of AMPA-selective glutamate receptor subunits in the entorhinal cortex of patients with Alzheimer's disease pathology: a biochemical study. Brain research 1995;678:161–167. [PubMed: 7542540]

Ye B, Zhang Y, Song W, Younger SH, Jan LY, Jan YN. Growing dendrites and axons differ in their reliance on the secretory pathway. Cell 2007;130:717–729. [PubMed: 17719548]

Yoon, T.; Okada, J.; Jung, MW.; Kim, JJ. Learning & memory. Vol. 15. Cold Spring Harbor, N.Y: 2008. Prefrontal cortex and hippocampus subserve different components of working memory in rats; p. 97-105.

Youn H, Jeoung M, Koo Y, Ji H, Markesbery WR, Ji I, Ji TH. Kalirin is under-expressed in Alzheimer's disease hippocampus. J Alzheimers Dis 2007a;11:385–397. [PubMed: 17851188]

Youn H, Ji I, Ji HP, Markesbery WR, Ji TH. Under-expression of Kalirin-7 Increases iNOS activity in cultured cells and correlates to elevated iNOS activity in Alzheimer's disease hippocampus. J Alzheimers Dis 2007b;12:271–281. [PubMed: 18057561]

Yuste R, Bonhoeffer T. Morphological changes in dendritic spines associated with long-term synaptic plasticity. Annual review of neuroscience 2001;24:1071–1089.

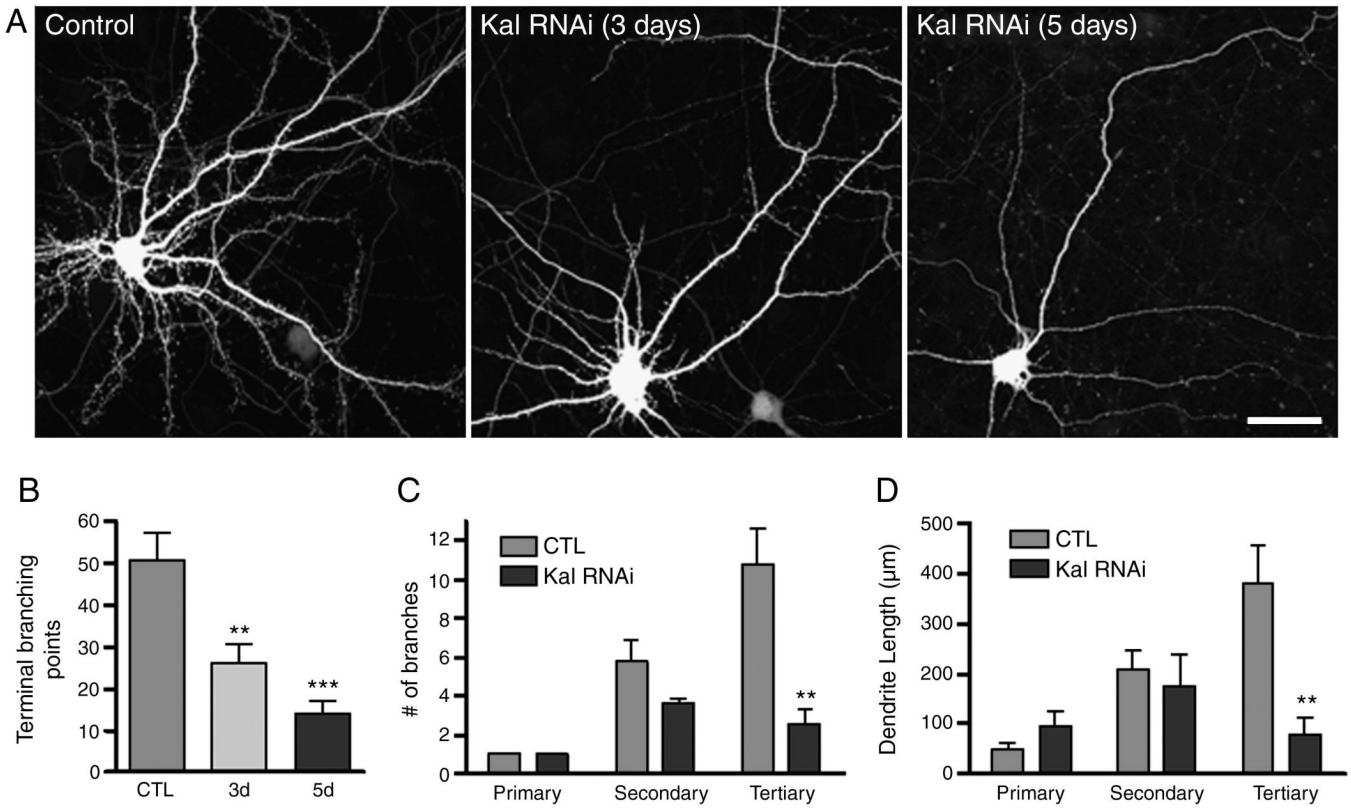

Fig. 1. Kalirin regulates dendritic morphology at neuronal level

(A) Time-dependent, progressive reduction of dendritic branching in cultured cortical pyramidal neurons where kalirin expression was knocked-down by RNA interference (Kal RNAi). (B) Quantification of terminal branching points after 5 days (5d) and 3 days (3d) of kalirin knockdown. The numbers (C) and lengths (D) of the primary, secondary, and tertiary dendrites after 5 days of kalirin knock-down. **, $p<0.01$; ***, $p<0.001$ compared with control (CTL). Scale bar: 20 μm.

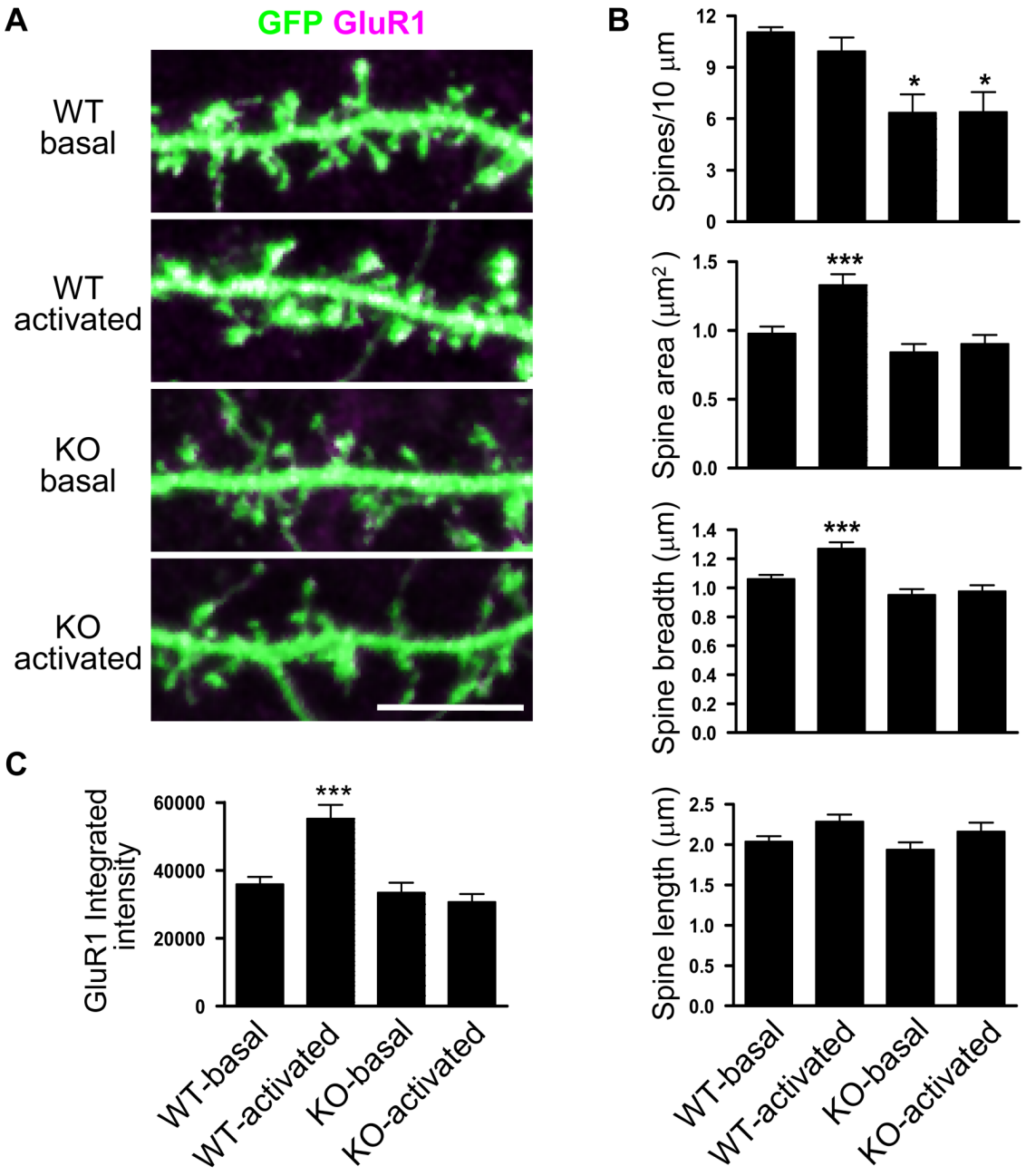

Fig. 2. Kalirin controls dendritic spine density and plasticity

(A) Cortical pyramidal neurons cultured from WT and KO mice were subjected to NMDA receptor activation for 30 min; neurons were expressing GFP (green) to show spine morphology; clustering of GluR1 subunits was revealed by immunofluorescence. White indicated overlapping of GluR1 and GFP. (B) Quantitative analysis of spine morphology parameters: spine linear density, spine area, spine breadth, and spine length. (C) Spine GluR1 clustering measured by the integrated intensity of GluR1 immunofluorescence. *, $p<0.05$; ***, $p<0.001$ compared with WT-basal. Scale bar: 10 μm.

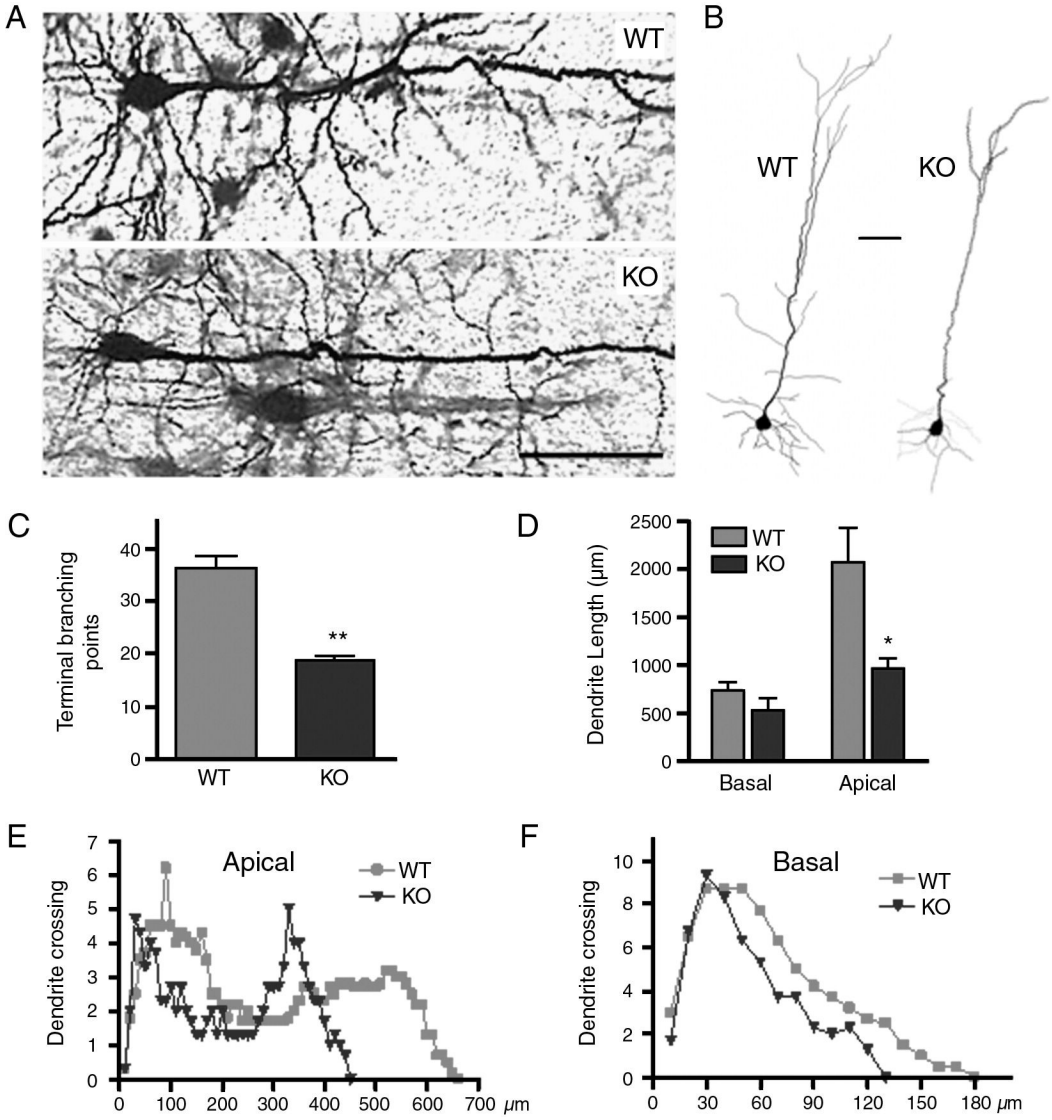

Fig. 3. Dendritic morphology of pyramidal neurons in *KALRN* KO mice

(A) Representative images of Golgi-stained layer 5 pyramidal neurons from the frontal cortices of WT and KO mice. (B) Representative 2-D projections of Neurolucida tracing of layer 5 pyramidal neurons in WT and KO frontal cortices. Neurolucida tracings were used to quantify terminal branching points (C), dendritic lengths (D), and Sholl analysis for all dendrites (E) and basal dendrites (F). *, $p<0.05$; **, $p<0.01$ compared with WT. Scale bars: 50 µm.

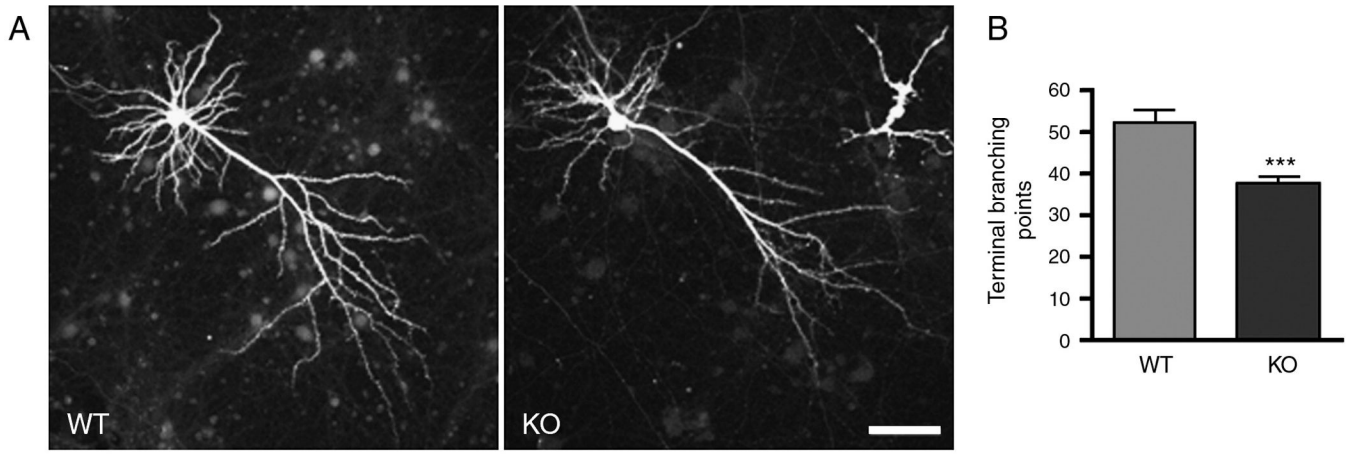

Fig. 4. Dendritic morphology of cultured *KALRN* KO pyramidal neurons

(A) Morphology of cultured cortical pyramidal neurons (DIV 28) from WT and KO mice was visualized by the expression of GFP. (B) Quantification of terminal branching points in A. ***, $p<0.001$. Scale bar: 50 μm.

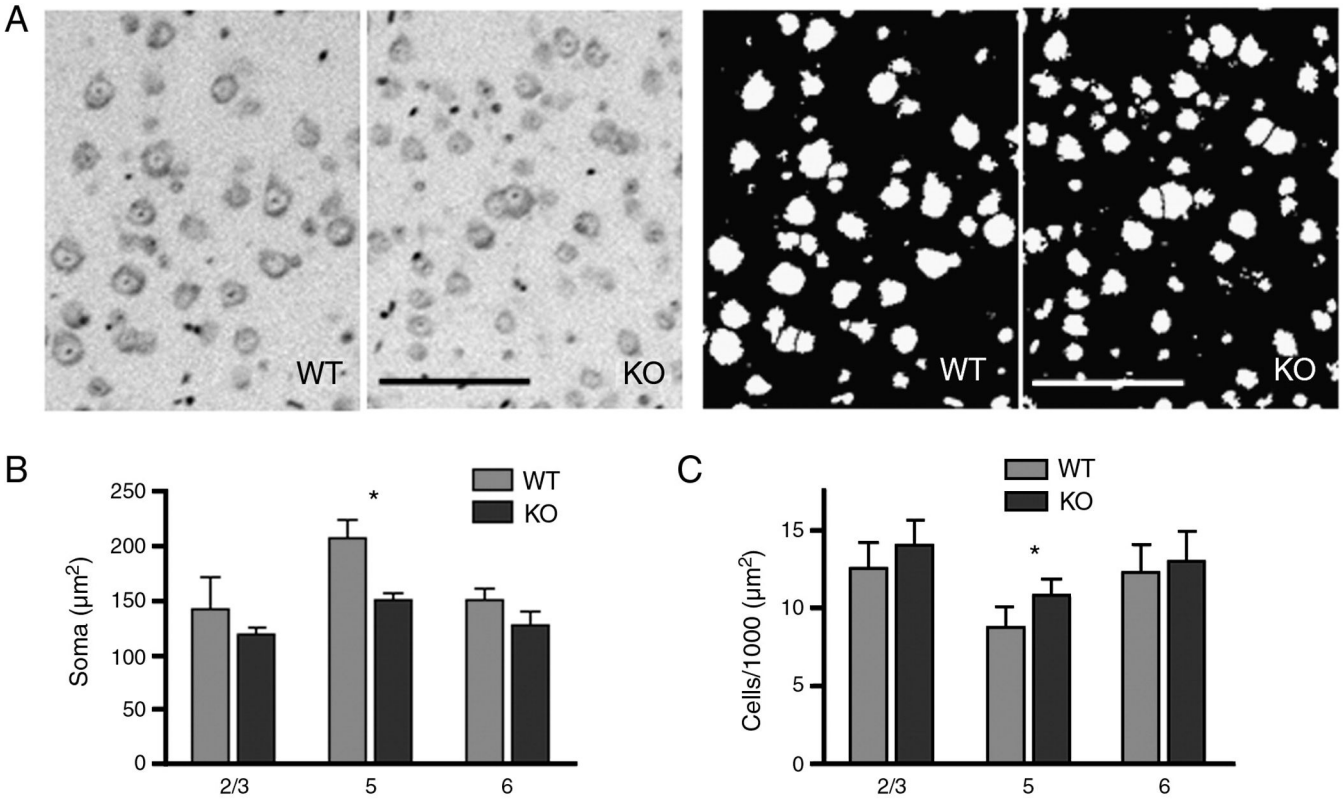

Fig. 5. Cytoarchitectural changes in the cortex of *KALRN* KO mice

(A) Left panel, representative images of Nissl stained layer 5 neurons in WT and KO frontal cortices; Right pane, image masks generated in Metamorph for the quantification of soma size and number from images on the left panel. Quantitative analysis of cell body sizes (B) and cell densities (C) in layers 2/3, 5, and 6 of WT and KO mice frontal cortices. *, $p<0.05$. Scale bar: 100 μm.

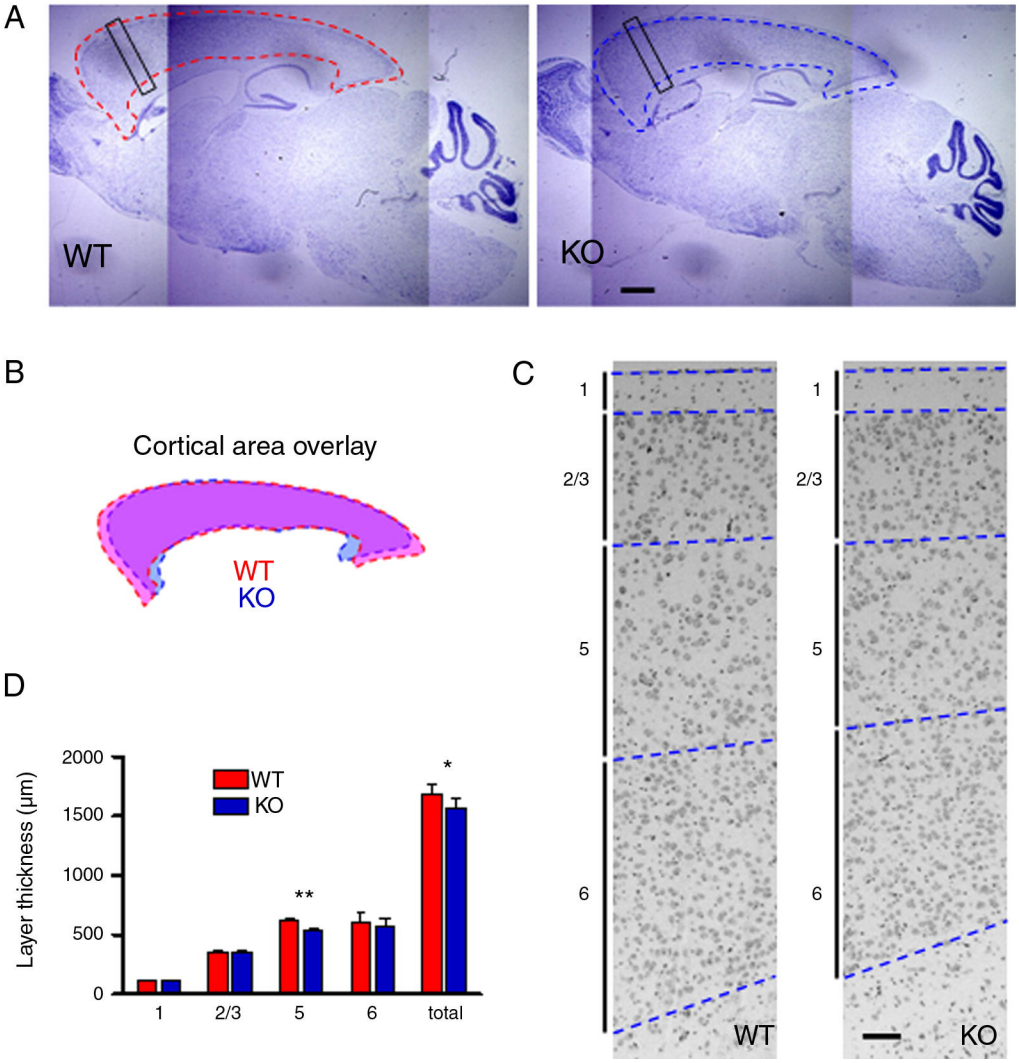

Fig. 6. Morphological changes in the cortex of *KALRN* KO mice

(A) Nissl stained sagittal sections of WT and KO brain; dashed lines delineate cerebral cortices. Black rectangular boxes indicate the frontal cortex regions analyzed in C–D. (B) Overlay of the WT (pink) and KO (light blue) cortical areas outlined in A. (C) Comparison of the WT and KO frontal cortices; the laminar structures in this part of the cortex were identified and represented by a vertical bar with a number corresponding to the respective layer. The borders between cortical layers were delineated by blue dashed lines. (D) Thickness of cerebral cortex layers in WT and KO frontal cortices. *, $p<0.05$; **, $p<0.01$. Scale bars: 1 mm (A); 100 μm (C).